Performance Analysis of Mini Wind Turbine Concept

Mahmood Jamal Al-Obaidi, Prof. Dr. Muna Sabah Kassim

ABSTRACT
Wind turbines are commonly used in renewable energy to produce green power energy, there are two types of wind turbine (horizontal and axial), and each one of them have their own usage. The goal of this project is to develop and build a non-conventional turbine. A (1.2 m) long wind tunnel with a (0.38 m) inner diameter was planned and built for the experimental section. The ideal place for the turbine turned out to be in the 1m part, with air speed of (10 m/s).The goal of this project is to develop and build a non-conventional turbine. An experimental wind tunnel was planned and built using local materials. The duct is manufactured from (2 mm) thick Perspex (transparent) material. A panel with a size of (600×1200 mm) was folded. An extraction fan of diameter 600 mm was used to produce an air velocity of 10 m/s.A team of researchers at the University of Aberdeen in Scotland has developed a new type of wind turbine that can be placed on the chimneys of an electric power plant. The difference reflects the increase in the amount of velocity entering the air stream over the velocity generated at the end of the turbine. In Case W11.5, a voltage of 12.5V was reached on the same ampere inverter, with the value of losses in the mechanical parts reaching 11.25 W and 13.52 W.

I. INTRODUCTION

The global trend of technical growth encourages the pursuit of the best solutions. The goal of more and practical science is to mathematically explain processes and allow computer software to simulate several scenarios in order to discover the optimal solution. This review will go through how to manage a wind turbine using LABVIEW, as well as a number of numerical and experimental assessments.

The breeze sun-oriented power creating station was used as a showing apparatus for University of Northern Iowa Industrial Technology understudies finding out about sustainable power. The new LABVIEW module adds genuinely necessary continuous data on framework factors like breeze speed, wind course, ac power, ac/dc voltages, and flows. Numerous parts of information gathering, instrumentation, communicating, and writing computer programs were talked about in this work [1].The goal of this research was to create a software package that would allow for the optimization of wind turbine blades based on a variety of factors. The reason for wind turbine configuration was to get the best attainable power yield under specific meteorological conditions. One methodology for altering firmness and steadiness was to change the math of the cutting edge, albeit this could influence the breeze turbine's productivity [2].An optimization technique based on the application of the NSGA-II in conjunction with the implemented surrogate models was used. The accuracy sizing and simulation models were compared to three Pareto-optimal solutions. It's worth noting that this topic might be used as a starting point for researching design approaches based on model hybridization, such as Space Mapping Methods [3].The examination of approach for ascertaining the ideal size of a Wind framework is introduced in this work. Long haul wind speed information for every hour of the day was utilized. A common dwelling load in the south of Algeria (desert region) was picked as the framework's heap interest. They found that utilizing GA, they could find the best design of wind turbines in terms of total cost [4].Cutting edge Element Momentum Theory (BEM) is utilized to assemble a HAWT edge for a 300 kW even pivot wind turbine. The breeze tip speed proportion, ostensible breeze speed, and rotor width are all plan components to consider. For each basic constitution of the edge, BEM was used to decide the most extreme lift to drag proportion [5].The impact of different airfoil profiles blades on overall wind turbine performance were explored in this study. Using both Blade Element Momentum (BEM) theory and a computer software, an aerodynamic analysis tool for horizontal axis wind turbine blades was developed. For a given wind speed, constant

rotational speed, number of blades, and blade radius, the method was used to optimize blade geometry [6].The shape optimization of wind turbine blade design as air flows was examined in this paper. The purpose was to improve the efficiency of energy production for a specific site by amortizing the turbine manufacturing cost. To maximize the turbine efficiency for specific wind, the blade aerodynamic analysis combines a 3D CFD code with an optimization code, Hyper study [7].This study proposes a streamlining model for flat hub wind turbine rotor sharp edges. The model depends on the breeze speed dispersion work for a particular breeze site. Cutting edges for a 1.3 MW slow down controlled breeze turbine are planned utilizing the laid-out enhancement calculation. The created sharp edges have preferred streamlined execution over the current edges [8].The effectiveness and center point twisting snapshot of a 5MW breeze turbine rotor cutting edge in light of the NREL 5MW reference turbine were improved. Reduced flap wise bending loads and blade surface area were anticipated to equate to lower rotor costs as a result of material savings. The cost of energy (COE) objective function was specified as rotor cost ($) AEP (MWh/yr) where AEP was annual energy production [9].The application of CFD can efficiently show the complex flow associated with the roll up of tip vortexes and 3D flow at the root sections. Commercial CFD algorithms have a realistic application for even huge multi-megawatt wind turbine blade models, according to the current investigations. Because of its broad applicability and the universality of a Navier-Stokes solver, CFD offers a lot of potential for modeling off-design instances where standard design tools fail [10].The goal of this research was to create a self-starting vertical axis wind turbine (VAWT). The primary goal of the project was to reduce the expenses of CNC cutting the three aluminum blades. To aid in the design of the full-scale turbine, a model that performs turbine theory calculations was constructed. Three blade profiles were tested and evaluated in the wind tunnel at Dalhousie University over the winter break. It was determined that using a profile with a large lift at low speeds and passive pitching could be achieved. The final product stood around 3 meters tall, had a blade height of 1.5 meters, and diameter of 2.5 meters [11].The Darrieus rotor was based on the same concepts as the VWT rotor. The construction consisted of a top and bottom ring, rotated and was supported at the bottom ring. There may be more than four blades between the two rings. The most well-known technologies were discovered and explained in order to understand the behavior of a

VWT [12].This thesis outlines a method for optimizing the rotor of a Savonius vertical axis wind turbine automatically. The power coefficient (CP) of this rotor was calculated using computational fluid dynamics to analyze its variations (CFD). Three optimizations were carried out with the goal of maximizing the CP and minimizing the difference (CP dif). The former was accomplished by altering the rotor's shape profile, size, and TSR; the former was achieved by altering its diameter, shape, and tip speed [13].The formulation uses a multi-objective optimization technique to maximize mean aerodynamic performance while minimizing susceptibility to variations in wind conditions. A non-intrusive collocation approach is employed to quantify uncertainty, which is combined with a RANS solver for fluid flow. Genetic Algorithms are utilized to iteratively evolve section parameters toward optimal designs. The results suggest that the proposed methodology has the potential to be applied to the robust design of industrial devices [14].The product bladed reproduction results show that the breeze turbine works safely while applying the disappointment activity methodology. This paper infers the connection between the drag coefficient and the electrical force of the generator. The proficiency misfortune condition of running is acquainted with the cutting-edge maturing reproduction, as well as the control strategy that consolidates pitch control and generator force speed control [15].Ghent University laid out the Small Wind Turbine Field Lab to examine the weaknesses of present little wind turbines while likewise exhibiting their true capacity (SWT Field Lab). This field lab, which is situated in Ostend's inward harbor, can oblige up to 10 minuscule breeze turbines, with seven turbines previously partaking in field tests. The presence of an assortment of 'fascinating' vertical pivot wind turbines close by more standard flat hub wind turbines (HAWT) demonstrates that the market is as yet advancing [16].

The goal of this project is to develop and build a non-conventional turbine. A numerical model for the turbine will be created using FLUENT 19.0 under the ANSYS commercial packages. This turbine will also be built and tested for the first time as well. To justify its performance capabilities, the numerical and analytical results will be compared to the experimental data.

II.   METHODOLOGY
The system Geometry Where the turbine duct was designed using the oil works program, a program dedicated to precise engineering design,

where two models were used for the first case using a turbine with a fan with a diameter of 340 mm and a diameter of 380 mm and a distance of 1 m from the air entry area where the length of the duct was 1.2 m and this is in the first case where the entry speeds were different It ranges from 5 m/s to 20 m/s with a difference of 5 m/s as in Figure 4.1, where the second turbine fan was designed and added to the first to complete the second case, where the diameter of the fan was 300 mm, also with the same dimensions as the external air duct, and also with the same entry speed as in Figure 1.
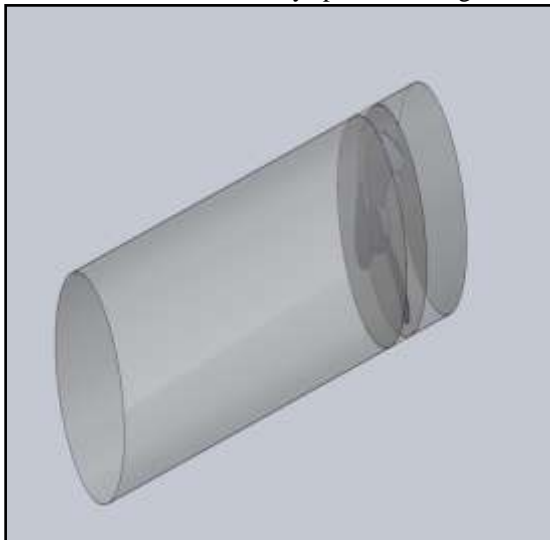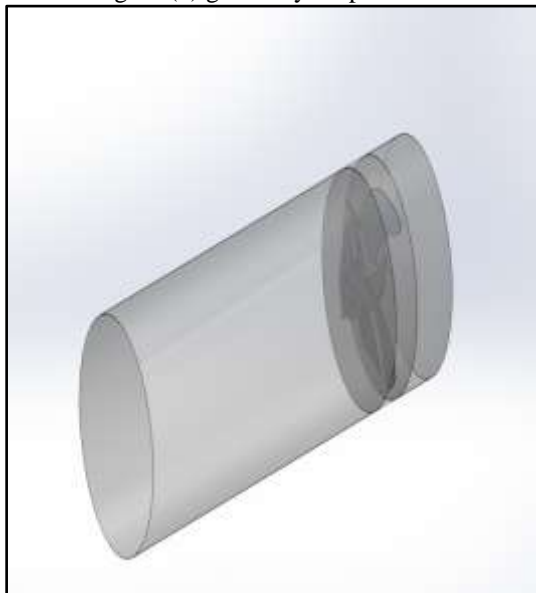

Figure (2) geometry shape case1.

Figure (2) geometry shape case2.

Mesh GenerationBy and large, unstructured matrices are effective for complex calculations, so for the above reason, the unstructured tetrahedron lattices was utilized in the current review.ANSYS support strong calculation network age and three-layered models with least contribution from a solitary stage from the client. The quantity of cells taken, in this study was (2065590) component, see figure (3).

Where we note that three different phases of the domain were used in each case, which represents the first region, the air access region to the second region containing the turbine, where the turbine rotates, and the third region represents the post-turbine region to the exit region.
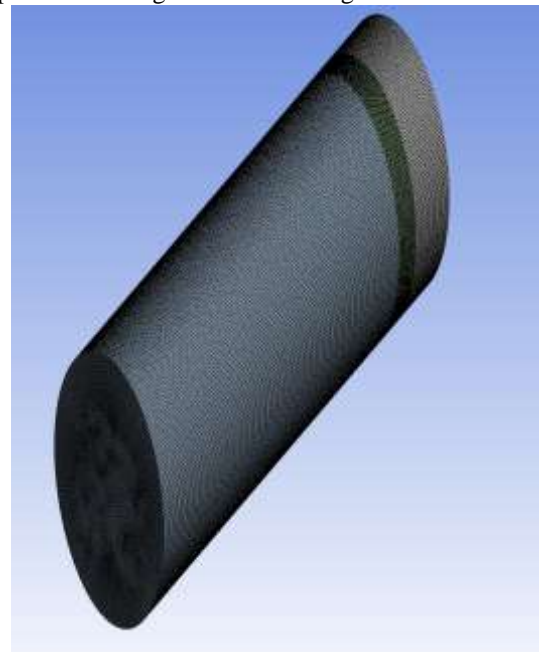

Figure (3) Mesh generated.

In order to obtain accurate results, it is necessary to work on the reliability of the mesh, through which it is possible to know the optimal solution for the simulation case, where the number of the element is increased to reach the state of induction in the results.

Table (1) Mesh independency.

case	element	node	force (N)
1	1223455	945323	8.25

2	1523323	1225456	8.51
3	1723543	1423567	8.58
4	2065509	1667109	8.59

The limits are somewhat dissimilar to from the trial and are organized at each of the three limit surfaces of the calculation area. Solid Wall BoundariesWhere the solid wall is the wall of the turbine to catch the air coming from the entry area. Inlet and Outlet BoundariesIn the current study, the inlet with the normal flow to the inlet level. velocity inlet and the entry velocity are at different speeds. As for the exit area, it is pressure outlet and its value is 0pa. Initial ConditionsThe stream field is obscure except if cycle is begun; along these lines, an underlying supposition is expected to begin the arrangement. For the current work, all factors are started from the channel limit conditions.Computational Fluid Dynamics (CFD) studies are performed to grow a more profound knowledge into the field of the stream. To explain the impact of the disturbance model which includes the arrangement of two vehicle condition, (k-ε) model is utilized. Subsequently, the strategies of the mathematical arrangement will settle these Cartesian direction frameworks (x, y, and z). Three-layered math is created.

III. GOVERNING EQUATIONS
The overseeing conditions to be addressed are the progression, force and the condition of the energy. The Mass Conservation Equation the condition for protection of mass, or coherence condition, can be composed as follows:

$$\frac{\partial \rho}{\partial t} + \nabla \cdot (\rho \vec{v}) = S_m \qquad (1)$$

the overall type of the mass protection condition and is legitimate for incompressible as well as compressible streams. The source S_m is the mass added to the ceaseless stage from the scattered second stage (for instance, because of vaporization of fluid beads) and any client characterized sources. For 2D axisymmetric calculations, the progression condition is given by

$$\frac{\partial \rho}{\partial t} + \frac{\partial}{\partial x}(\rho v_x) + \frac{\partial}{\partial r}(\rho v_r) + \frac{\rho v_r}{r} = S_m \qquad (2)$$

here x is the hub coordinate, r is the outspread direction, v_x is the hub speed, and v_r is the spiral speed.

Energy Conservation Equations Conservation of force in an inertial (non-speeding up) reference outline

$$\frac{\partial}{\partial t}(\rho \vec{v}) + \nabla \cdot (\rho \vec{v}\vec{v}) = -\nabla p + \nabla \cdot (\bar{\tau}) + \rho \vec{g} + \vec{F} \qquad (3)$$

where p is the static strain,$\bar{\tau}$is the pressure tensor (depicted underneath), and $\rho\vec{g}$ and $\vec{F}$ are the gravitational body power and outer body powers (for instance, that emerge from communication with the scattered stage), separately. $\vec{F}$ likewise contains other model-subordinate source terms, for example, permeable media and client characterized sources.

The pressure tensor $\bar{\tau}$is given by$\bar{\tau} = \mu\left[(\nabla\vec{v} + \nabla v T - \frac{2}{3}\nabla\cdot v I\right] \qquad (4)$

where μ is the sub-atomic thickness, I is the unit tensor, and the second term on the right-hand side is the impact of volume enlargement. For 2D axisymmetric calculations, the pivotal and spiral energy preservation conditions are given by

$$\frac{\partial}{\partial t}(\rho v_x) + \frac{1}{r}\frac{\partial}{\partial x}(r\rho v_x v_x) + \frac{1}{r}\frac{\partial}{\partial r}(r\rho v_r v_x) = -\frac{\partial p}{\partial x} + \frac{1}{r}\frac{\partial}{\partial x}\left[r\mu\left(2\frac{\partial v_x}{\partial x} - \frac{2}{3}(\nabla\cdot\vec{v})\right)\right] + \frac{1}{r}\frac{\partial}{\partial r}\left[r\mu\left(\frac{\partial v_x}{\partial r} + \frac{\partial v_r}{\partial x}\right)\right] + F_x \qquad (5)$$

and

$$\frac{\partial}{\partial t}(\rho v_r) + \frac{1}{r}\frac{\partial}{\partial x}(r\rho v_x v_r) + \frac{1}{r}\frac{\partial}{\partial r}(r\rho v_r v_r) = -\frac{\partial p}{\partial r}$$
$$+ \frac{1}{r}\frac{\partial}{\partial x}\left[r\mu\left(\frac{\partial v_r}{\partial x} + \frac{\partial v_x}{\partial r}\right)\right]$$
$$+ \frac{1}{r}\frac{\partial}{\partial r}\left[r\mu\left(2\frac{\partial v_r}{\partial r} - \frac{2}{3}(\nabla \cdot \vec{v})\right)\right] \quad (6)$$
$$- 2\mu\frac{v_r}{r^2} + \frac{2}{3}\frac{\mu}{r}(\nabla \cdot \vec{v}) + \rho\frac{v_z^2}{r} + F_r$$

where

$$\nabla \cdot \vec{v} = \frac{\partial v_x}{\partial x} + \frac{\partial v_r}{\partial r} + \frac{v_r}{r} \quad (7)$$

and v_z is the swirl velocity.

Transport Equations for the Standard k-ε ModelThe disturbance motor energy, k, and its pace of scattering, ε, are acquired from the accompanying vehicle conditions:

$$\frac{\partial}{\partial t}(\rho k) + \frac{\partial}{\partial x_i}(\rho k u_i) = \frac{\partial}{\partial x_j}\left[\left(\mu + \frac{\mu_t}{\sigma_k}\right)\frac{\partial k}{\partial x_j}\right] + G_k +$$
$$G_b - \rho\varepsilon - Y_M + S_k \quad (8)$$

and

$$\frac{\partial}{\partial t}(\rho\varepsilon) + \frac{\partial}{\partial x_i}(\rho\varepsilon u_i) = \frac{\partial}{\partial x_j}\left[\left(\mu + \frac{\mu_t}{\sigma_\varepsilon}\right)\frac{\partial\varepsilon}{\partial x_j}\right] +$$
$$C_{1\varepsilon}\frac{\varepsilon}{k}(G_k + C_{3\varepsilon}G_b) - C_{2\varepsilon}\rho\frac{\varepsilon^2}{k} + S_\varepsilon \quad (9)$$

In these situations, Gk addresses the age of disturbance motor energy because of the mean speed angles, determined as depicted in Modeling Turbulent Production in the k-ε Models). Gb is the age of choppiness active energy because of lightness, determined as portrayed in Effects of Buoyancy on Turbulence in the k-e Models acting dilatation in compressible choppiness to the general

dissemination rate, determined as depicted in EffectsofCompressibilityon Turbulencein the k-e and σ_ε are the fierce Prandtl numbers for k and ε, separately. S_k and S_ε are client characterized source terms. Modeling the Turbulent Viscosity,the turbulent (or eddy) viscosity, $\mu_{t'}$, is computed by combining k and ε as follows:

$$\mu_t = \rho C_\mu \frac{k^2}{\varepsilon} \quad (10)$$

where C_μ is a constant. Model ConstantsThe model constants $C_{1\varepsilon}, C_{2\varepsilon}, C_\mu, \sigma_k$, and σ_ε have the following default values:

$$C_{1\varepsilon} = 1.44, C_{2\varepsilon} = 1.92, C_\mu = 0.09, \sigma_k = 1.0, \sigma_\varepsilon = 1.3$$

IV.   EXPERIMENTAL WORK

The development of the experimental apparatus used to test the design is covered in this chapter. It is vital to test the turbine design experimentally in order to ensure that it is correct. The first section of the chapter describes in detail the system and processes utilized to carry out the experimental work, as well as the system's components. The description of the interface unit follows, while the steps of experimental testing and instrument calibration are covered in the second section.

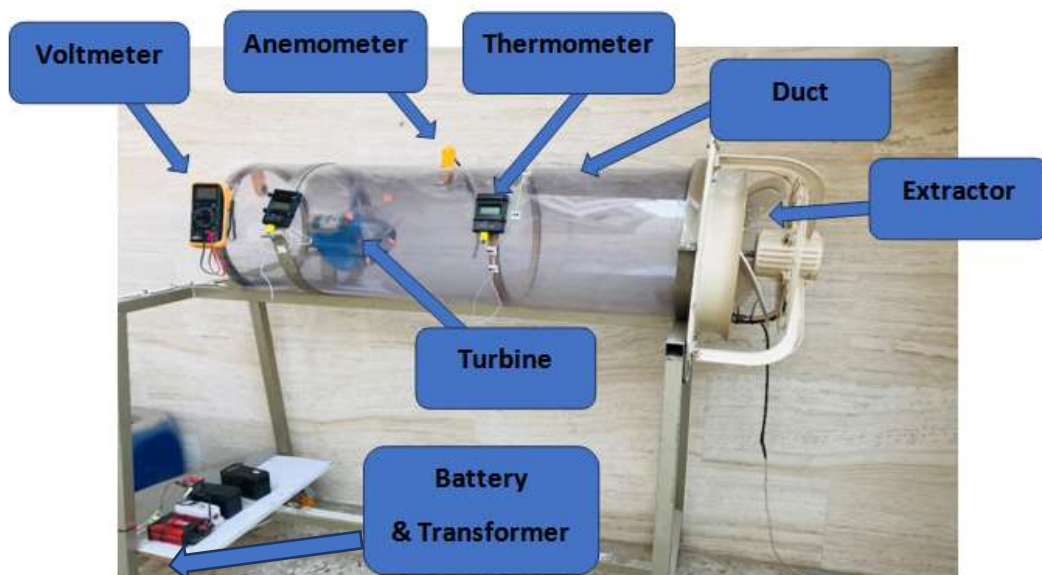The figure (4) reveals the experimental rig which are comprises of the following components.

Figure (4): The Component of the Rig

This project's goal is to use wind to test the turbine that has been built and manufactured. Because the scope of this project does not include determining the maximum available wind in Iraq, a wind tunnel has been developed in its place. In the local market, an experimental wind tunnel was planned and built using local materials. The following are the elements that make up this system.

The duct is manufactured from (2 mm) thick Perspex (transparent) material. A panel with a size of (600×1200 mm) was folded. The constructed duct has a diameter of 380 mm and a length of 1200 mm.Extraction Fan An extraction fan of diameter 600 mm was used to produce an air velocity of 10 m/s. The fan with 360 W.The measuring DevicesIt wind Velocity Measurement (Analog)An anemometer was used to measure the Velocity of Air inside the tunnel before and after the turbine. The device is bought from market with ± 0.1 m/s of error, as mention on it.K-Type Thermometer (Analog)A tow K-Type thermometer was used to measure the temperature inside and outside the duct, with error (±0.1 ^{0} C). Voltmeter (Analog)An analog Voltmeter was used to measure the voltage gained from the generator of the wind turbine. The Turbine components are collected from local markets, the first fan (with blue color) and second fan is a handmade fan (with clear color) as shown in figure (5).

Figure (5): Turbine fan shape.

This design made to improve the speed of the turbine in the same air speed from the extraction fan installed. The turbine was fixed in the duct with distance of 1000 mm of the extraction fan. The turbine was attached to a generator shown in figure (3.3).Generatorwe used in this research a generator of 24 Volt and 0.9 Ampere capacity, connected to a battery to charge it with the wind turbine energy which connected to an amplifier to change the 24 V to 220 V to produce electricity for turning on a lamp connected to the system directly as in figure (6).

Figure (6): The Generator.

Electrical Devicesone battery and one amplifier used to charge and produce the electricity from the wind turbine.

Experimental workIt is as followsMake all the assembled rig together.Put all the measuring devices in place.Fix the turbine.Turn on the power for extractor fan so we have air inside the duct with max velocity of 10 m/s.Wait for the turbine to self-turn by the air velocity inside the duct.Turn on all the measuring devices to measure the velocity the voltage and temperature also.Wait for the battery to be charged enough so we can turn on the amplifier to get lamp on.All these steps are done for the first fan (blue one) only to see the difference between it and with adding the handmade one to it.Turn off the power and add the handmade fan to the blue one.Start over again and see the differences between two fans.

V. RESULTS AND DISCUSSION
5.1Results of experimental work

In this research work, we choose the wind speed according to what we have available in the local market. Which is within the limits of 10 m/s.

first attempt we put the blue fan, the output wind speed 5.5 m/s so the efficiency (η) is:

$$\eta = \frac{\text{output wind speed}}{\text{input wind speed}} \times 100$$

$$\therefore \eta = \frac{5.5}{10} = 0.55\ \%$$

In this attempt we found that the output voltage reach to 11.5 V.

While in the second attempt by using clear color fan with blue fan together, the output wind speed 7 m/s so the efficiency became:

$$\therefore \eta = \frac{7}{10} = 0.70\ \%$$

In this attempt we obtain 12.5 V, from this results we can found that our enhancement percentage (μ):

$$\mu = \frac{\text{output voltage in second attempt}}{\text{output voltage in first attempt}} \times 100$$
$$\therefore \mu = \frac{12.5}{11.5} = 1.087\ \%$$

From above results we found that this enhancement is used for decrease the charge time for the battery. So we will have more time in which use it to turn on our load for longer time, also we will increase the life of the battery used in this system., use this system (model) which is designed for special cases to find the efficiency (η) about 0.79 % which is approximately to our enhanced system design in attempt two when we use the clear color fan and blue fan together.in this research work in our design we put the clear color fan in front of the blue fan as shown in figure (3:2) instead of behind as we expect that the wind will not completely hit the clear color fan in this case we lose part of the wind energy.

5.2 Results of numerical work

In this section, the results obtained from the numerical part, i.e., obtained from the CFD simulation program, will be reviewed, discussed, and narration of the effects caused by the velocity of air entry, as well as the presence of an additional turbine that was added to increase the efficiency of converting air energy into electrical energy.

5.2.1 The effect of air flow velocity on the amount of pressure generated by the turbine

The increase in the speed of air flow helps to increase the pressure generated on the surfaces of the turbine and thus increases its ability to rotate. We note through the following figures that the increase in the value of the air flow speed increases the pressure generated on the surfaces of the turbine and thus increases its rotational speed as four speeds were used Changing the air to see this change.
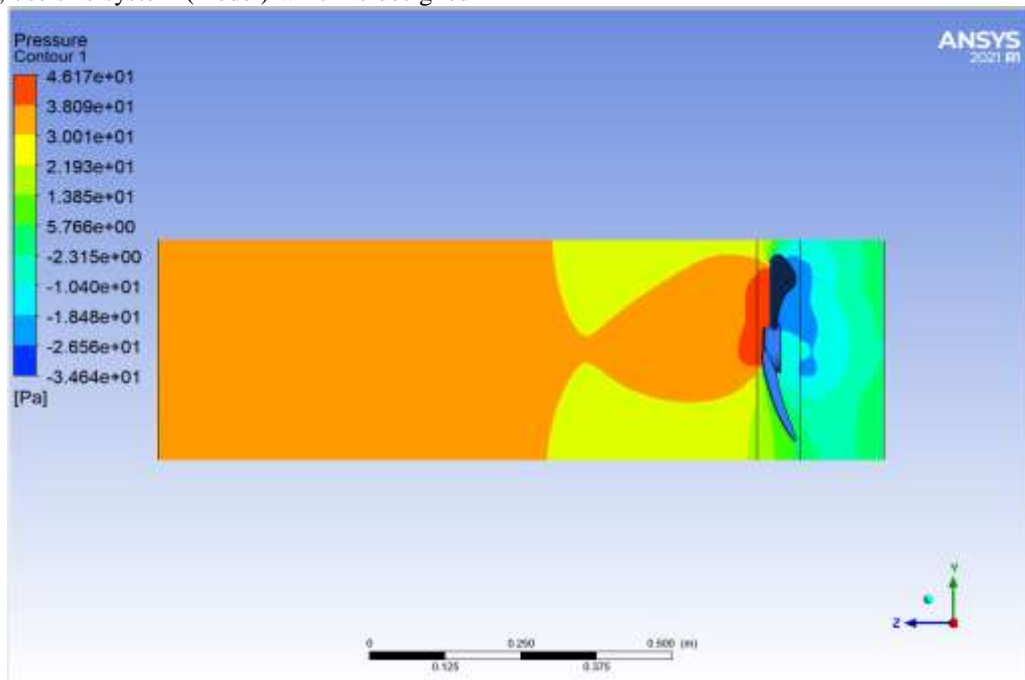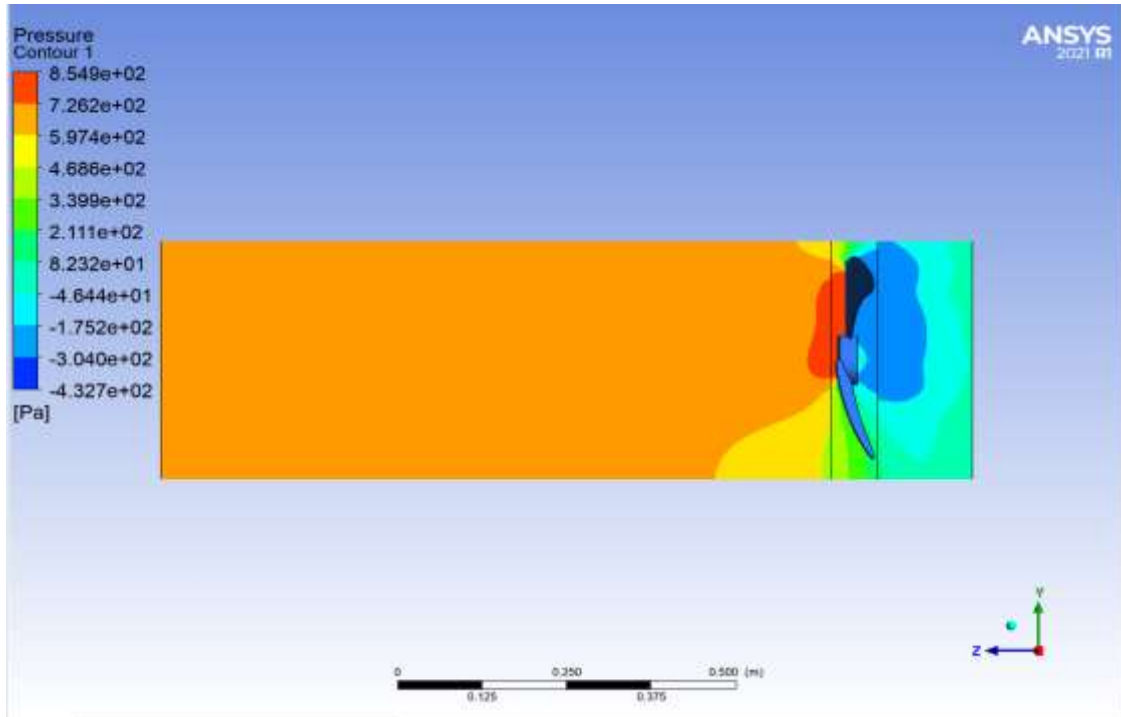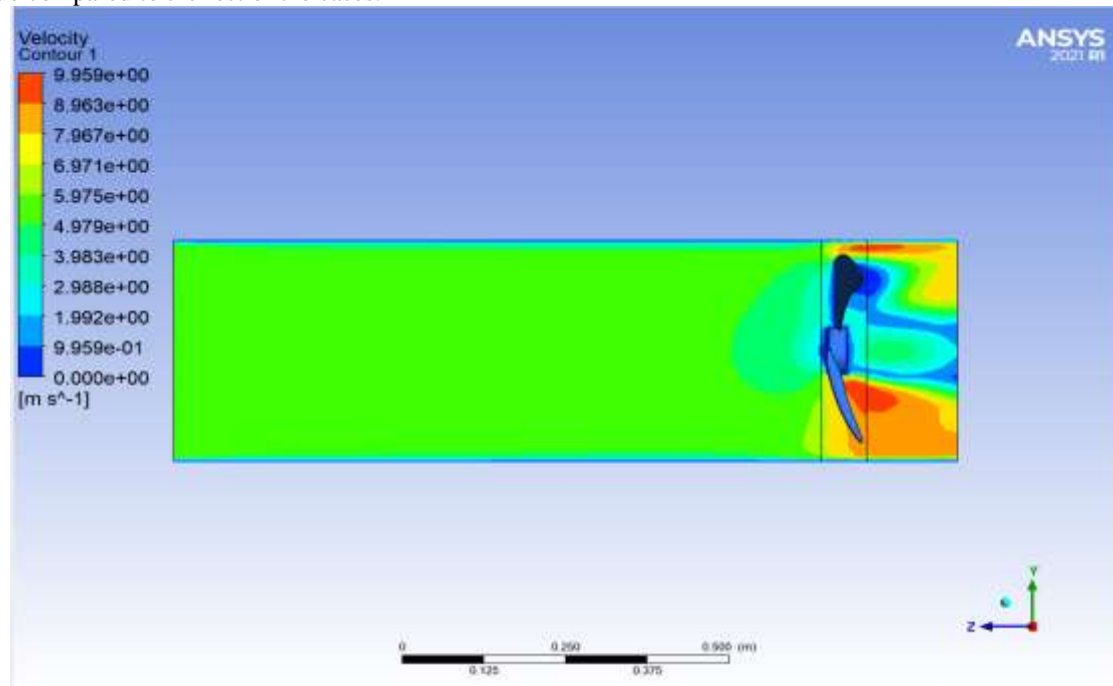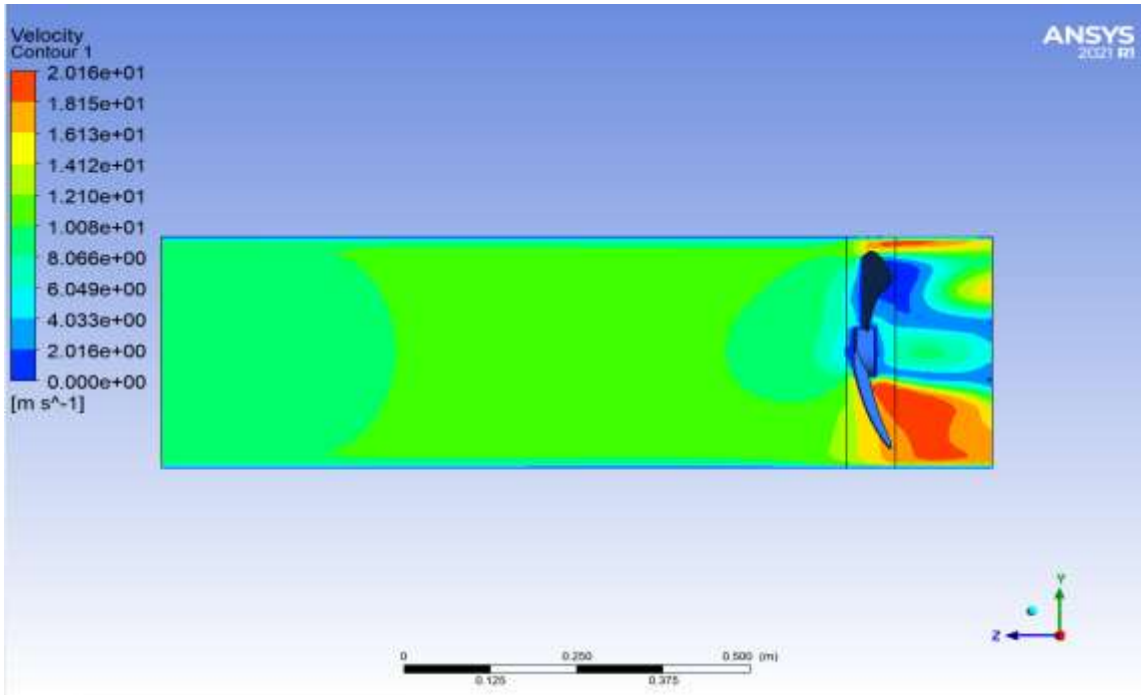

(a)
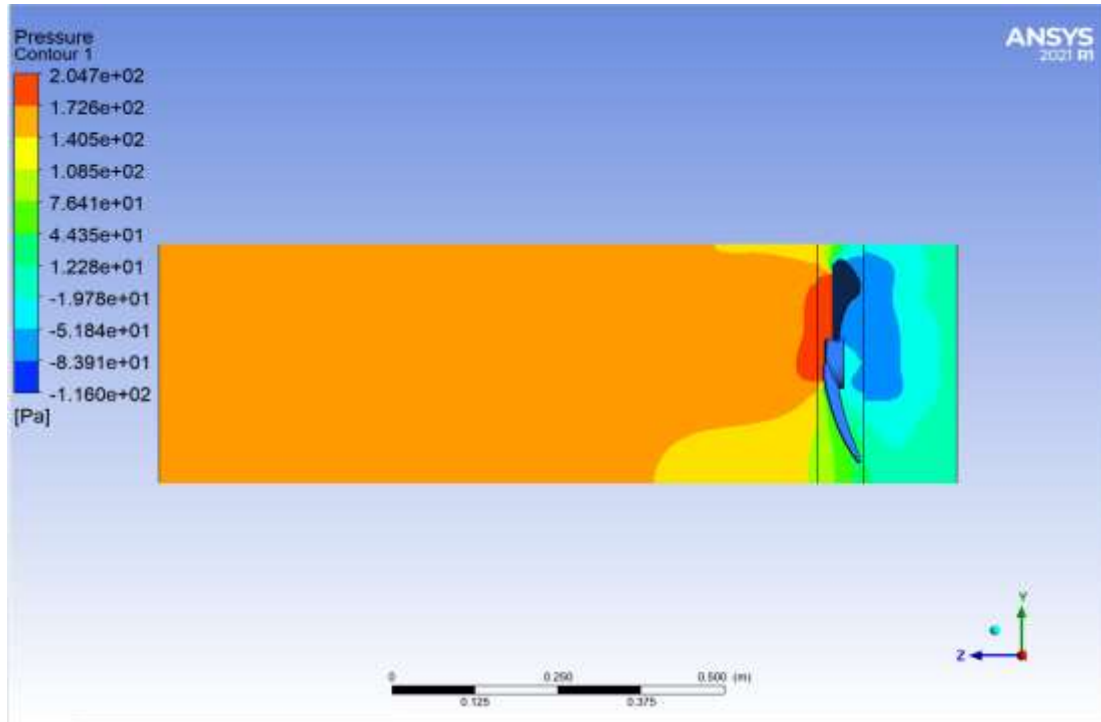
(b)
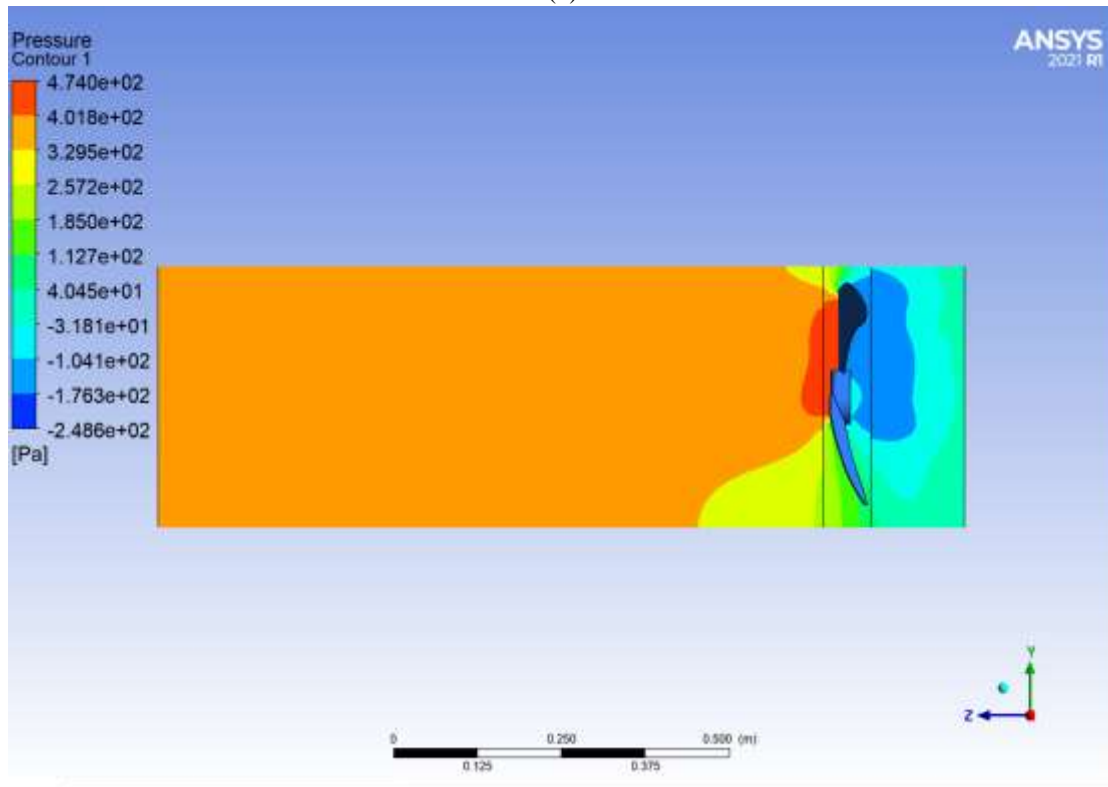
(c)

(d)

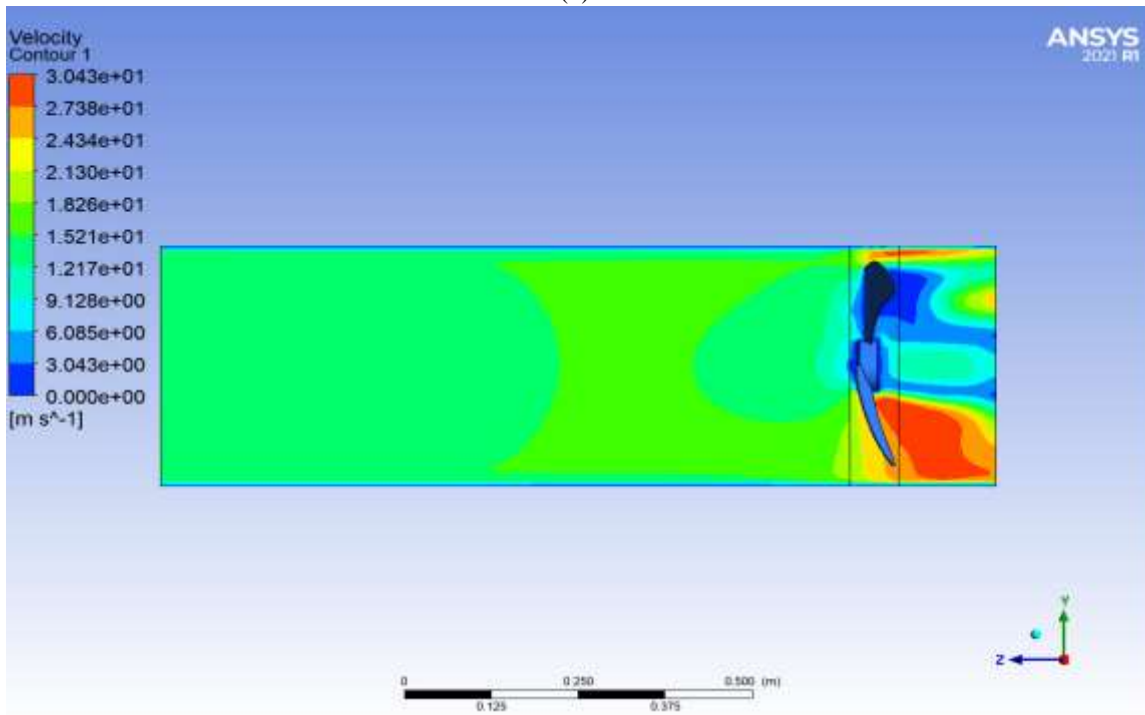Figure (7) pressure contourcase1. (a)5m/s, (b)10m/s, (c)15m/s, (d)20m/s.

Where we note through the previous figures that the pressure value began to increase with the increase in the value of the air entry velocity, reaching 854pa at an entry velocity of 20 m/s, which is the highest-pressure value compared to the rest of the cases.
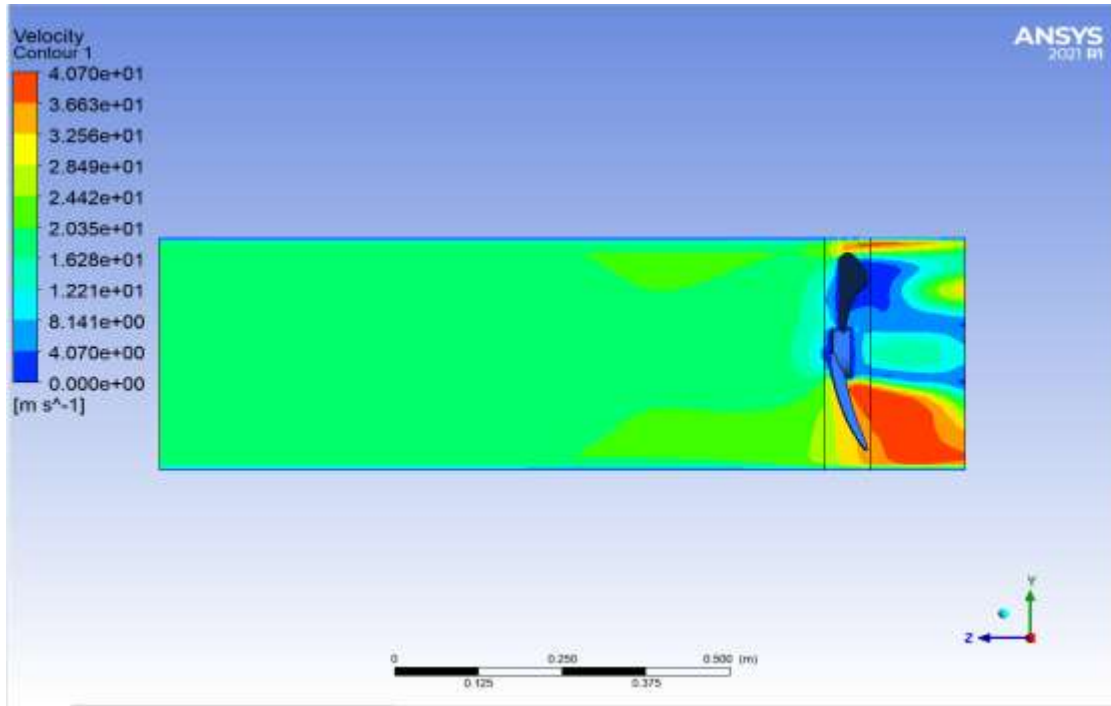

(a)

(b)

(c)

(d)

Figure (8) velocity contourcase1. (a)5m/s, (b)10m/s, (c)15m/s, (d)20m/s.

As for the forms of air flow velocity values, we notice the clear difference from the increase in the amount of velocity entering the air stream over the velocity generated at the ends of the turbine. We note through the previous figures that the air flow velocity at the ends of the turbine reached 40 m/s in the case in which the air inlet velocity is 20 m/s.

5.2.2 The effect adding an extra turbine fanon the amount of pressure generated by the turbine

The addition of an additional turbine fan increases the shock pressure as a result of the passage of air on it and thus increases the rotational speed of the turbine. We note through the previous figures that the pressure value increases with an increase in the number of used turbines.
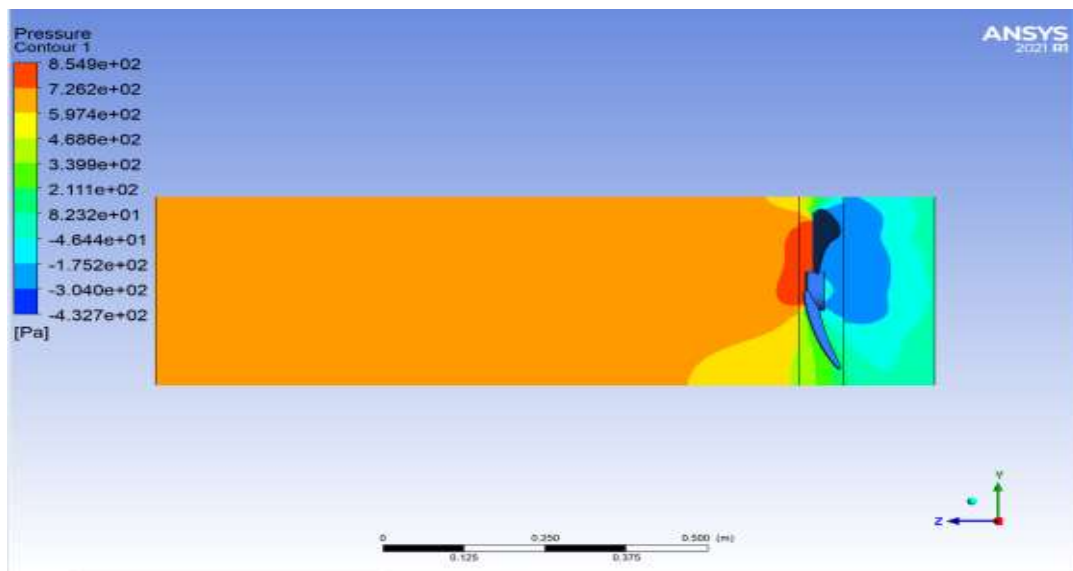

(a)
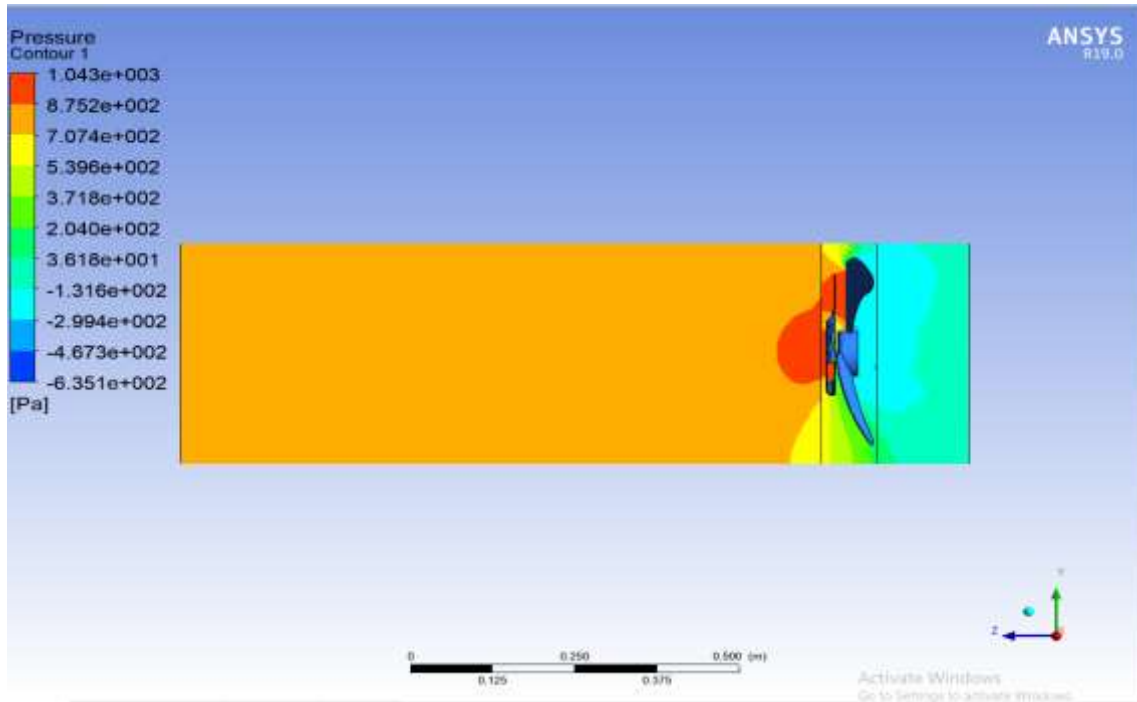
(b)
Figure (9) pressure contour. (a)cace1, (b)case2.

Where we notice from the previous figures that the value is significantly and sloppy, as the pressure value reached 1043pa when adding a turbine in addition to the case in which the air entry velocity is 20m/s, which is the largest pressure value obtained compared to the rest of the cases, which contributes to spinning the turbine with greater torque and value spinning more.

5.2.3 The effect adding an extra turbine fanon the amount of pressure generated by the turbine
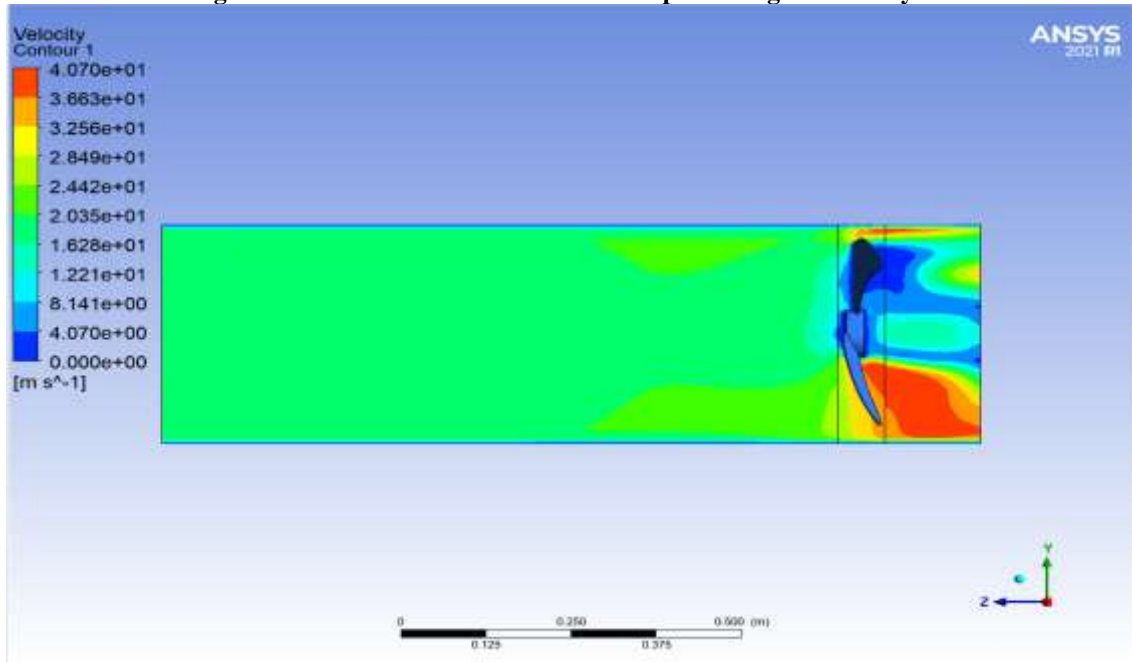
(a)
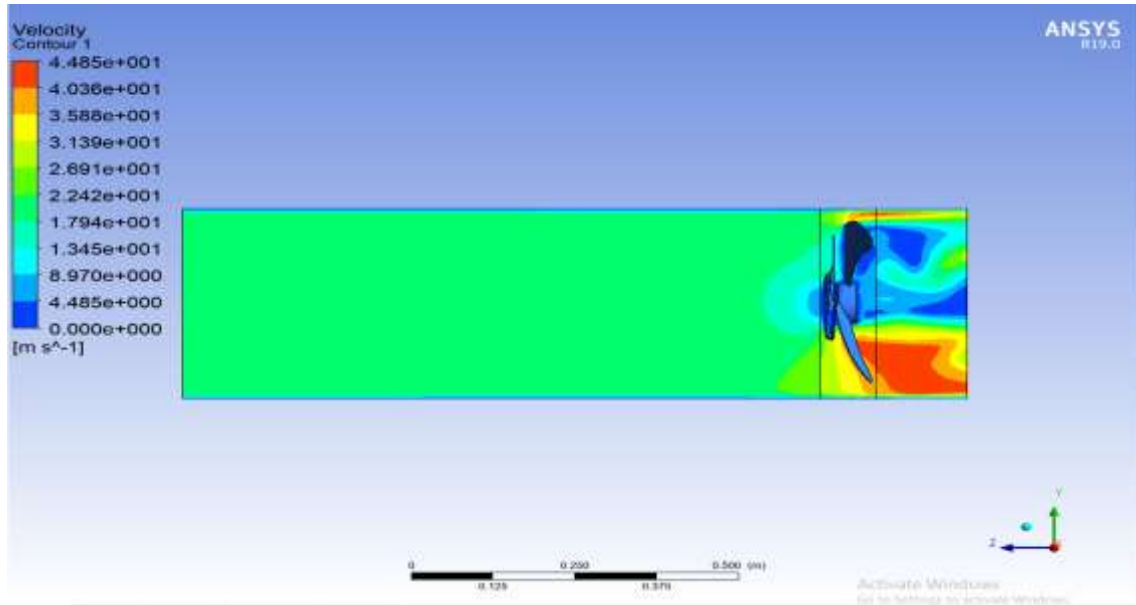
(b)
Figure (10) velocity contour. (a)cace1, (b)case2.

As for the value of the airflow velocity at the ends of the turbine, even if the airflow velocity is used when entering the same in both cases, the value of the air flow velocity at the tips of the turbine when adding another turbine increases significantly as the airflow velocity at the ends of the turbine reached 44m/s in the case that is It has an air inlet velocity of 20m/s.

5.2.4 The amount of power output from the turbine

The increase in the velocity of the air entering air from the entry area increases the forces acting on the turbine walls and thus increases its rotation speed and the torque used. The amount of energy extracted from the turbine rotation can be calculated as in the following table:

Table (2) Power calculation of case1.

inlet velocity (m/s)	moment (N.m)	angular velocity (rad/s)	Power (W)
5	0.2622192	10.47197551	2.745953041
10	1.0747572	10.47197551	11.25483108
15	2.438508	10.47197551	25.53599606
20	4.354476	10.47197551	45.59996604

Where the turbine's rotational speed was fixed, the amount of torque that was extracted from the simulation program was calculated, and the amount of energy generated by the turbine was calculated. We note that the value of the power reached 45.5w when the air entry velocity was 20 m/s.

Table (3) Power calculation of case2.

inlet velocity (m/s)	moment (N.m)	angular velocity (rad/s)	Power (W)
5	0.3833412	10.47197551	4.014339659
10	1.577652	10.47197551	13.52113311
15	3.581268	10.47197551	37.5029508
20	6.393012	10.47197551	66.94746511

Where we note that when adding the other turbine, it increases the torque significantly, and thus the value of the resulting power increases, as the power reached 66w, which is the largest amount of power that can be reached compared to the rest of the cases, which is at the speed of air entry 20m/s.
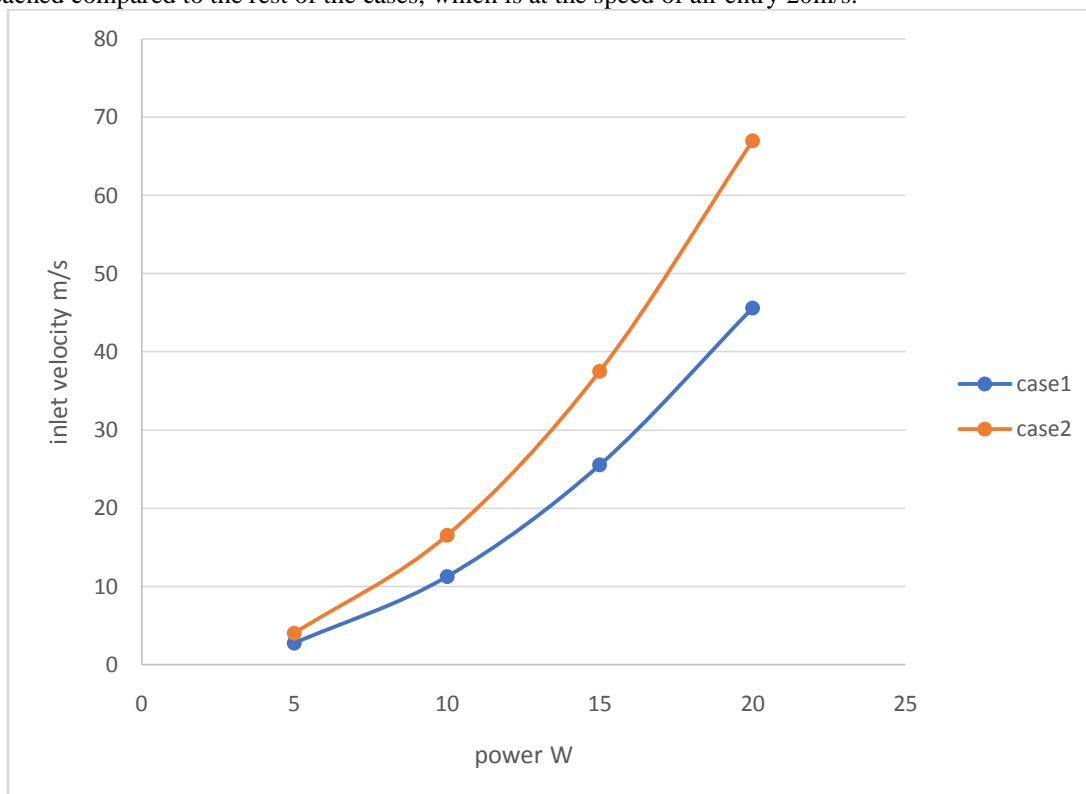

Figure (11) Power with inlet velocity of air.

Through the previous figure, we note the significant impact of the presence of the additional turbine, which increased the amount of energy extracted and thus increases the value of the efficiency between the electrical energy, which represents the input energy and the mechanical energy, which represents the output energy.

5.2.5 Comparison between the experimental part and the numerical part

One of the most important reasons for the simulation process for the real case is a comparison between simulation and experimental work, which helps in understanding the correct way to work and how close we are to its validity. (5, 10, 15 and 20) m/s for both cases, where the comparison will be made at the speed that was taken, as the comparison value lies in the output energy of the

two cases, where at the speed of 10m/s in the first case, the output voltage reached 11.5v on the inverter whose ampere value is 1A, as the value of the energy in this Case W11.5 As for the numerical part, the mechanical energy was obtained, which is supposed to be similar to the amount of electrical energy, with the value of the losses in the mechanical parts reaching 11.25 W, which is logical In the second case, a voltage of 12.5V was reached on the same ampere inverter, in which the power is 12.5W. In the numerical work, in the second case, at the speed of 10m/s, the value of the mechanical power was reached to 13.52W, which is very logical and close to experimental work.

VI.   CONCLUSION

A team from the University of Aberdeen in Scotland has designed a system that can be placed on chimneys of an electric power plant to increase its production of electricity and reduce the cost of producing electricity by using artificial wind turbines, according to their own research. The system (rig) is made up of materials that bought from local markets with law cost (about 1000000 IQD) while turbine cost about (100000 IQD), whereas the price of artificial turbine is about 450000 IQDs.Air flow velocity at the ends of a wind turbine reaches 40 m/s in the case in which the air inlet velocity is 20m/s, compared to the previous figures for the air outlet velocity. The difference reflects the increase in the amount of velocity entering the air stream over the velocity generated at the end of the turbine.The value of power reached 45.5w when the air entry velocity was 20 m/s and the speed of the turbine was set to 20m/s, as shown in the figure below. Where the turbine's rotational speed was fixed, the amount of torque that was extracted from the simulation program was calculated.In Case W11.5, a voltage of 12.5V was reached on the same ampere inverter, with the value of losses in the mechanical parts reaching 11.25 W and 13.52 W, which is very logical and close to experimental work. At the speed of 10m/s, at the same inverter an output voltage of 11.5v was reached - this is similar to theoretical work.

REFERENCES

[1]. Pecen, R., Salim, MD., and Zora, A. " A LabView Based Instrumentation System for a Wind-Solar Hybrid Power Station" the Official Electronic Publication of the National Association of Industrial Technology, Auqust, V20, 2004.

[2]. Jureczko, M., Pawlak, M., and M,e˙zyk, A., " Optimisation of wind turbine blades" Journal of Materials Processing Technology , 2005.

[3]. Abdelli, a., Sareni, b.,andRoboam, x., "Optimization of a Small Passive Wind Turbine Generator with Multiobjective Genetic Algorithms" International Journal of Applied Electromagnetics and Mechanics, 2007.

[4]. Benatiallah,A., Kadi,L., Dakyo, B.," Modelling and Optimisation of Wind Energy Systems " Jordan Journal of Mechanical and Industrial Engineering, Jordan, January,2010.

[5]. Mirhosseini, m., Alaian,m., Sedaghat, a., and Alemrajabi, a., "Aerodynamic design of a 300 KW horizontal axis wind turbine" Isfahan University of Technology, Iran, September, 2011. 69

[6]. Rathore , A., and Ahmed, S., " Aerodynamic Analyses of Horizontal Axis Wind Turbine By Different Blade Airfoil Using Computer Program" IOSR Journal of Engineering, 2012.

[7]. Moissiadis, A., Paschaloudis, D., Tsioraklidis, L., " Aerodynamic Shape Optimization of Wind Turbine Blades" Lecture Notes in Information Technology, Vol.13, 2012.

[8]. Xiong. L., Yan, C., Zhiquan, Y., Optimization model for rotor blades of horizontal axis wind turbines" Mech. Eng. China 2007.

[9]. Richard,W., Vesel, J., "Aero-Structural Optimization of a 5 MW Wind Turbine Rotor" The Ohio State University,2012.

[10]. Jesper, L. Peder, E. and Søren, H., "3D CFD rotor computations of a Multimegawatt HAWT rotor " IOP Publishing,2007.

[11]. DeCoste, J., McKay, D., Robinson, B., Whitehead, S., and Wright, S., " Vertical Axis Wind Turbine" Dalhousie University, December 5, 2005.

[12]. Jorgensen, T., and Nielsen, H.," Vertical Wind Turbine" Aarhus University, Denmark, December, 2008.

[13]. Acevedo, J .," Optimization of the efficiency of a Savonius wind turbine for urban media using a genetic algorithm" CAMPUS MONTERREY, Spain, December, 2008. 69

[14]. Tachikawa, H., Schiavazzi, D., Arima, T., and Iaccarino, G.," Robust optimization for windmill airfoil design under variable wind conditio", Stanford University, 2012.

[15]. Zhang,L., Sun, Y., and XiangzhouLv " Design on Pitch-control Wind Turbine

System Based on Bladed" Chinese Control and Decision Conference (CCDC), 2011.

[16]. Laveyne,J.I., De Kooning, J., Wyngene, K. V., and Ackere, S. V., " The Small Wind Turbine Field Lab" Publisher: Institutional repository - Gent University, 2013.

[17]. Boubaker, O."National Instruments® LabVIEW™: Ultimate Software for Engineering Education" National Institute of Applied Sciences and Technology, Tunis, Tunisia.

[18]. Rainieri,C., Fabbrocino, G. and Cosenza, E., "Implementation of omaprocedures Using LABVIEW:theory and application" Department of Structural Engineering - University of Naples "Federico II", Italy.

[19]. Rocha, I., Veloso, A.C., Carneiro, S., Costa, R. and Ferreira ,C.,"Implementation of a specificratecontrollering FED-BATCH E. coli fermentation" published research for Seoul, Korea, July 6-11, 2008.